Opto-Electronic Advances

Supplementary information

February 2023, Vol. 6, No. 2

DOI: 10.29026/oea.2023.220012

Highly efficient vectorial field manipulation using a transmitted tri-layer metasurface in the terahertz band

Huan Zhao[1,2], Xinke Wang[2], Shutian Liu[1]* and Yan Zhang[2]*

[1]Department of Physics, Harbin Institute of Technology, Harbin 150001, China; [2]Beijing Key Laboratory of Metamaterials and Devices, Key Laboratory of Terahertz Optoelectronics, Ministry of Education, Beijing Advanced Innovation Center for Imaging Theory and Technology, Department of Physics, Capital Normal University, Beijing 100048, China.

*Correspondence: ST Liu, E-mail: stliu@hit.edu.cn; Y Zhang, E-mail: yzhang@cnu.edu.cn

This file includes:

Supplementary information for this paper is available at https://doi.org/10.29026/oea.2023.220012

Section 1: Numerical simulation of electric field distributions of the unit cell

Figure S1 shows the numerical simulation of electric field distributions in the unit cell #1. The incident wave is *x*-polarized and the transmitted light is *y*-polarized. The white dashed lines indicate the positions of metallic structures. Figure S1(a) shows the distribution of E_x field, one can see almost all the E_x field is localized near the C-shaped antenna in the middle layer and therefore it can be effectively transformed to its cross polarized E_y field. Figure S1(b) shows the distribution of E_y field. It can be found that the E_y field is radiated from the C-shaped antenna and passes the bottom *x*-direction metagrating directly.

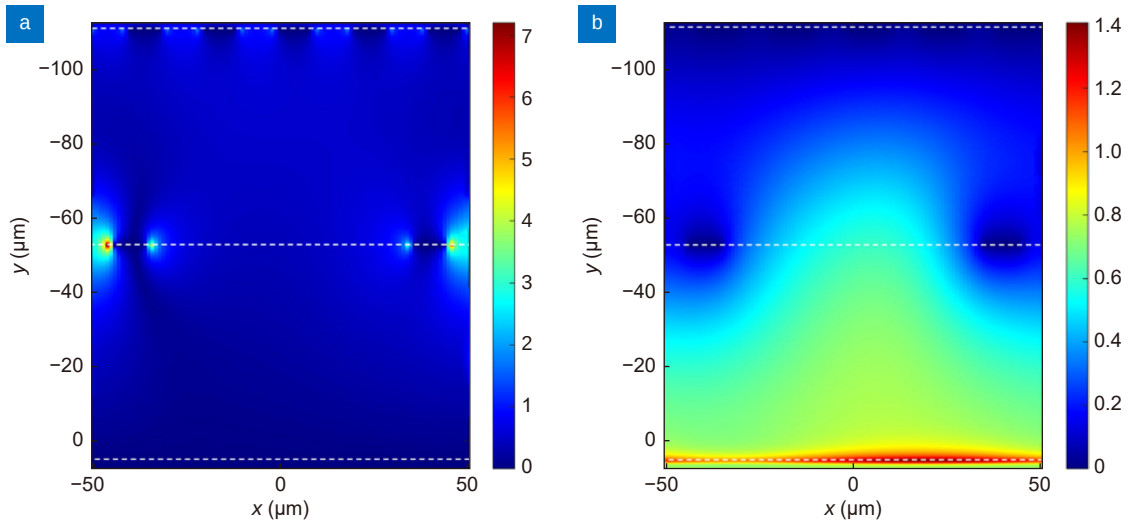

Fig. S1 | Numerical simulations of (**a**) E_x and (**b**) E_y field distributions for the unit cell #1, The incident wave is *x*-polarized and the transmitted light is *y*-polarized. The white dashed lines indicate the positions of metallic structures.

Section 2: Jones matrix of the designed tri-layer metasurface

The designed metasurface consists of a tri-layer metallic structure. The top and bottom layers are orthogonal metagratings that serve as polarizers with angles θ+90° and θ, respectively. The middle layer is a C-shaped antenna array that modulates the phase of the transmitted θ-polarized wave (depending on the opening angle 2α of the antenna). Therefore, the Jones matrix of the unit cell of the metasurface can be expressed as:

$$\mathbf{J}=\begin{bmatrix}\sin^2\theta & -\frac{1}{2}\sin2\theta\\ -\frac{1}{2}\sin2\theta & \cos^2\theta\end{bmatrix}\cdot\begin{bmatrix}0 & t_{xy}e^{i\varphi_{xy}(\alpha)}\\ t_{yx}e^{i\varphi_{yx}(\alpha)} & 0\end{bmatrix}\cdot\begin{bmatrix}\cos^2\theta & \frac{1}{2}\sin2\theta\\ \frac{1}{2}\sin2\theta & \sin^2\theta\end{bmatrix}, \tag{S1}$$

where (t_{xy}, φ_{xy}) and (t_{yx}, φ_{yx}) represent (amplitude transmission, phase modulation) of the metasurface, and the first and second subscripts represent the polarization states of the incident and transmitted waves. Because the C-shaped antenna is axially symmetric, (t_{xy}, φ_{xy}) and (t_{yx}, φ_{yx}) have the relationships t_{xy}=t_{yx} and φ_{xy}=φ_{yx}+π. Inserting these relationships into Eq. (S1) gives:

$$\begin{aligned}\mathbf{J}&=t_{xy}e^{i\varphi_{xy}(\alpha)}\cdot\begin{bmatrix}\cos^2\theta & \frac{1}{2}\sin2\theta\\ \frac{1}{2}\sin2\theta & \sin^2\theta\end{bmatrix}\cdot\begin{bmatrix}0 & 1\\ -1 & 0\end{bmatrix}\cdot\begin{bmatrix}\sin^2\theta & -\frac{1}{2}\sin2\theta\\ -\frac{1}{2}\sin2\theta & \cos^2\theta\end{bmatrix}\\ &=t_{xy}e^{i\varphi_{xy}(\alpha)}\cdot\begin{bmatrix}-\frac{1}{2}\sin2\theta & \cos^2\theta\\ -\sin^2\theta & \frac{1}{2}\sin2\theta\end{bmatrix},\end{aligned} \tag{S2}$$

where the polarization state is determined by the angle θ, which also denotes the direction of the metagrating. The phase modulation is a function of the opening angle 2α of the C-shaped antenna. Therefore, the polarization angle and phase of the transmitted wave can be modulated individually by tuning the angles θ and 2α.

Section 3: Evaluation of the working efficiency

In the simulation, the field monitors were set to record the electric fields E_x, E_y, and E_z in the frequency range from 0.1 to 1.5 THz. The working efficiency is defined as:

$$\eta=\sqrt{\frac{I_{\text{out}}}{I_{\text{in}}}}\ , \tag{S3}$$

where I_{out} and I_{in} are the integrated total intensities of the transmitted and incident waves, respectively, at one specific frequency.

For the experiment, a uniform metasurface was designed and fabricated with 100×100 identical cells. The direction angle θ was selected as 90°, and antenna #1 was adapted in the middle layer. The sample could transfer the incident x-polarized wave to the output y-polarized wave with a uniform phase modulation. A home-built THz focal-plane imaging system was used to characterize the performance of the fabricated metasurface. The complex amplitudes of the illuminating x-polarized wave and transmitted y-polarized wave were recorded. Then, the working efficiency spectrum was calculated as the amplitude of the transmitted wave divided by that of the illuminating wave. The same method was used to calculate the working efficiency of the THz vectorial hologram.

Section 4: Phase and polarization modulation of the THz polarization analyzer

The phase modulation of the THz polarization analyzer was designed to be a lens characterized by:

$$\phi(x,y)=\frac{2\pi}{\lambda}(f-\sqrt{x^2+y^2+f^2})\ , \tag{S4}$$

where λ=400 μm is the incident wavelength, and f is the focal length, which is 10 mm in the design. The phase was constrained to the range from 0 to 2π and quantized to eight values, as shown in Fig. S2(a). Meanwhile, the polarization modulation was designed to have an azimuthal distribution, as shown in Fig. S2(b).

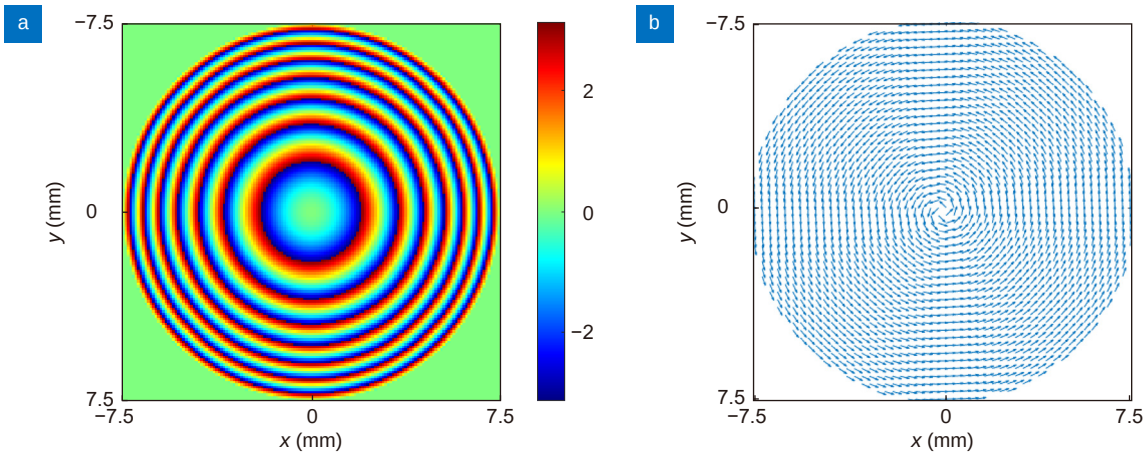

Fig. S2 | (**a**) Phase and (**b**) polarization modulation distributions of the designed THz polarization analyzer.

Section 5: Simulated annealing algorithm and phase distribution of the THz vectorial hologram

The simulated annealing (SA) algorithm was used to calculate the phase distributions of the holograms, and then the phase distributions were used to arrange each basic unit. In the SA algorithm, the exponential temperature curve was set as:

$$t(k)=t_0\times aq\ , \tag{S5}$$

where t_0 is the initial temperature, which was set as 200; q is the iteration number; and a is the cooling temperature ratio, which was set as 0.995 in the optimization. In each iteration, the Rayleigh–Sommerfeld diffraction was used to calculate the optical field $U_2(x_2, y_2)$ on the image plane from the optical field $U_1(x_1, y_1)$ on the source plane:

$$U_2(x_2,y_2)=\frac{1}{\mathrm{j}\lambda}\iint U_1(x_1,y_1)\cdot\frac{\exp\left(\frac{\mathrm{j}k}{2}\sqrt{d^2+{x_1}^2+{y_1}^2}\right)}{d^2+{x_1}^2+{y_1}^2}\mathrm{d}x_1\mathrm{d}y_1\ , \tag{S6}$$

where (x_1, y_1) and (x_2, y_2) are the coordinates of the source plane and image plane, respectively; d=1.5 mm is the

distance between the source and image planes; λ is the working wavelength; and k is the corresponding wave vector. After 2500 iterations, stable holographic images with high quality were obtained. Figure S3(a) presents one of the desired images: number 2 in channel 2. The simulated amplitude of the reconstructed image is shown in Fig. S3(b), and the phase modulation of the corresponding metasurface is shown in Fig. S3(c).

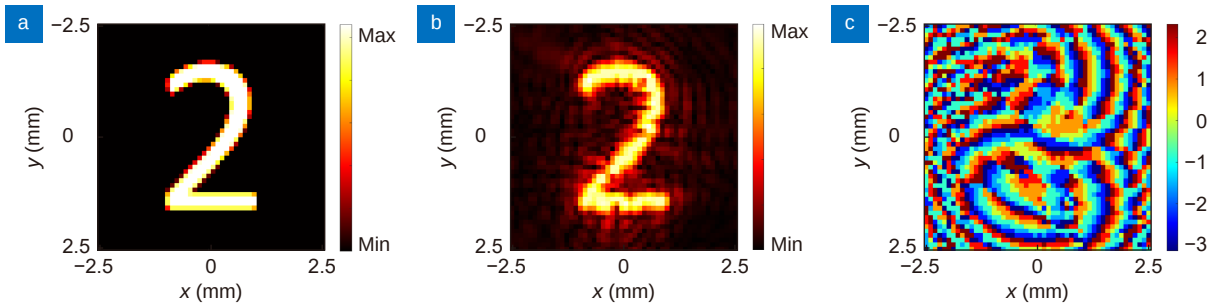

Fig. S3 | (**a**) Desired object image number 2 in channel 2. (**b**) Reconstructed amplitude distribution of the hologram. (**c**) Phase modulation of the corresponding metasurface.

Section 6: Characteristics of the THz focal-plane imaging system

Figure S4(a, b) show the time-domain signal and frequency-domain spectrum of the THz wave generated for the THz focal-plane imaging system, respectively. The duration of the THz pulse is about 2 ps, while the frequency range is approximately 2 THz.

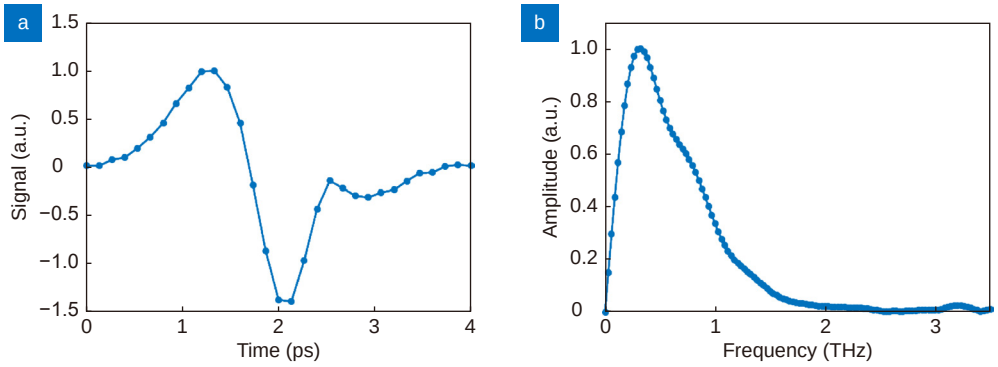

Fig. S4 | (**a**) Time-domain signal and (**b**) frequency-domain spectrum of the THz focal imaging system.

The amplitude distribution of the THz beam at 0.75 THz is shown in Fig. S5(a). The diameter of the spot is approximately 1.5 cm. The amplitude along the white dashed line in Fig. S5(a) is extracted and shown in Fig. S5(b). The amplitude distribution of the THz beam is Gaussian, which affects the hologram imaging quality.

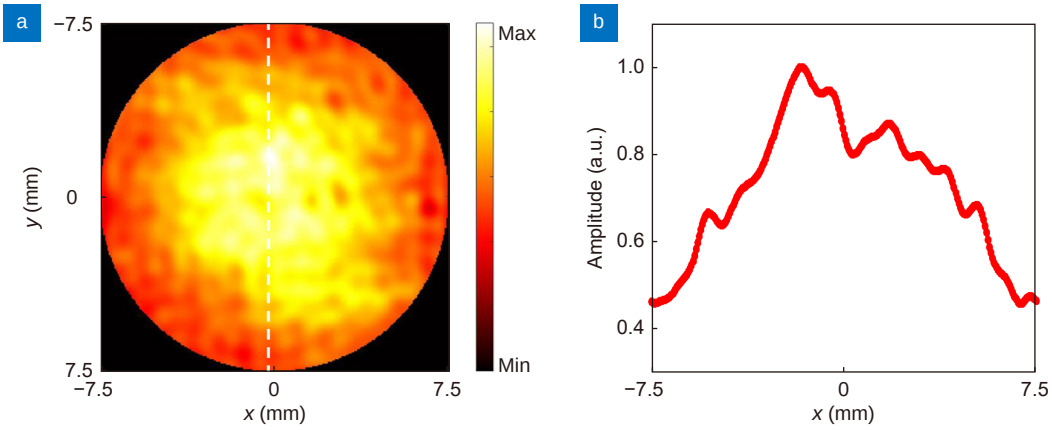

Fig. S5 | (**a**) Measured amplitude distribution of the illuminating wave at 0.75 THz. (**b**) Amplitude distribution extracted along the white dashed line in (a).